

# Event-Triggered Finite-Time Consensus Scheme for Time-Delay Multi-Agent Systems with Settling Time Estimation and its Application

Haini Zhang<sup>1</sup> , Ding Zhou<sup>2\*</sup> 

1. Jiangsu Vocational Institute of Commerce  – School of Finance – Nanjing – China.

2. Purple Mountain Laboratories  – Endogenous Security Research Center – Nanjing – China.

\*Correspondence author: zhouinghawk@163.com

## ABSTRACT

This study addresses the finite-time formation control issues associated with time-delay multi-agent systems. To tackle the challenges of finite-time stability in delay systems, Artstein's transformation is utilized. A distributed finite-time consensus algorithm is developed, incorporating an event-triggered control scheme and a corresponding triggering function to minimize unnecessary energy consumption and reduce the frequency of controller updates. The validity of the proposed approach is rigorously established through Lyapunov stability theory and finite-time stability theory, ensuring the absence of Zeno behavior. Furthermore, building upon the finite-time consensus algorithm, a finite-time formation control algorithm is formulated, enabling a group of agents to follow a designated leader while maintaining a specified formation shape. By employing feedback linearization, the unmanned aerial vehicle model is transformed into a precise linearized model. Finally, the application of this framework to formation control is presented, demonstrating the effectiveness of the proposed results.

**Keywords:** Aerospace systems; Time delay; Feedback control; Automatic flight control.

## INTRODUCTION

In recent decades, the consensus of multi-agent systems has attracted considerable interest within both academic and industrial research communities. This field primarily focuses on the cooperative control of interconnected agents to establish and maintain a predetermined configuration. Agents operating in formation are capable of executing complex missions, including disaster monitoring, target encirclement, and military surveillance (Amirkhani and Barshooi 2022). Given the wide range of applications, numerous studies have been conducted to develop and implement formation control algorithms for various types of unmanned vehicles (Ahmed *et al.* 2022; Gargalakos 2024; Ni *et al.* 2021; Yakıcı *et al.* 2024). Several formation control strategies are available, including such as leader-follower, behavior-based, and virtual rigid body approaches, which encompass two distinct control frameworks: the centralized structure and the distributed structure. Notably, the consensus-based control method has emerged as the predominant strategy due to its simplicity and reliability in implementation. This approach has led to a wealth of significant research contributions, further advancing the field and providing valuable insights for future developments (Mikaberidze *et al.* 2024; Zhang *et al.* 2022).

Received: Aug. 5, 2024 | Accepted: Jan. 6, 2025

Peer Review History: Single Blind Peer Review.

Section editor: Paulo Renato Silva 



Based on the consensus algorithm, many research results can be found for formation control (Dou *et al.* 2022; Huang *et al.* 2021a). It is noteworthy that consensus-based algorithm are expected to reach a goal when time approaches infinity. Achieving finite-time consensus is significant in practical systems, especially in high-speed systems (Luo *et al.* 2024; Wang *et al.* 2023). As a result, the convergence rate has become a critical performance metric for assessing the effectiveness of formation control protocols. This aspect is gaining increasing attention within the field. In contrast to asymptotic convergence algorithms, finite-time control protocols offer significant advantages, including faster convergence speeds and enhanced disturbance rejection capabilities (Liu *et al.* 2022). These improvements make finite-time approaches particularly appealing for practical applications in formation control. Numerous finite-time formation control algorithms have been developed to address the challenges in this area (Huang *et al.* 2021b; Shou *et al.* 2022). These algorithms are specifically designed to enhance convergence speed and robustness, making them suitable for a variety of applications in formation control.

It is essential to acknowledge that the finite-time formation control algorithms previously discussed employ continuous-time control methodologies. This strategy necessitates that the controller perpetually refresh its control inputs, potentially resulting in considerable energy expenditure. Such frequent updates are particularly impractical for unmanned vehicles, which typically rely on embedded microprocessors and have limited energy resources (Wang *et al.* 2022; Znidi and Nouri 2024). To address this issue, event-triggered control has emerged as a promising alternative. This control paradigm minimizes the need for continuous updates, thereby optimizing energy consumption while maintaining effective control performance (Gong *et al.* 2023; Yang *et al.* 2021). Inspired by the event-triggered strategy, researchers have progressively directed their attention towards the implementation of event-triggered schemes in the context of formation control (An *et al.* 2023; Hou and Lu 2022; Wen *et al.* 2023; Yang *et al.* 2020). These developments underscore the potential of event-triggered control strategies to improve the efficacy of formation control systems.

In the aforementioned studies on event-triggered formation control (Li *et al.* 2024; Xie *et al.* 2024), it is posited that each vehicle operates without accounting for the time delays associated with information transmission and processing, which appears unrealistic in practical use. To tackle this issue, various methodologies have been investigated for spacecraft (Liu *et al.* 2017) and unmanned underwater vehicles (UUVs) (Xu *et al.* 2023). The research in Liu *et al.* (2017) involved the formulation of control protocols that utilize rapid terminal sliding manifolds and switching functions. However, these protocols only considered time delays within the sliding mode, which may render them impractical in real-world applications. Building on the work in Xu *et al.* (2023), the research presented in Romero *et al.* (2023) introduced a finite-time protocol specifically designed for non-holonomic robots encountering time delays. This approach requires significantly large control parameters to ensure stability. In practical situations, such large parameters may exceed the actuator's capabilities and jeopardize stability. To the best of our knowledge, a limited body of research exists on finite-time event-triggered formation control schemes that account for time delays.

The primary contribution of this paper can be articulated as follows: 1) The application of integral transformation is utilized to tackle the finite-time stability issues inherent in delay systems; 2) The event-triggered control scheme is employed to reduce the necessity for constant updates to the controller. In this approach, the controller is updated only when a triggering event occurs, significantly reducing energy expenditure; 3) A more precise estimation of finite settling time is obtained through a careful construction of the Lyapunov function. Through the application of feedback linearization, the model of an unmanned aerial vehicle (UAV) is converted into a precise linearized representation. This approach is employed in the context of UAV formation control to illustrate the efficacy of the outcomes.

## Preliminaries

### *Lemma 1* (Nie *et al.* 2023)

Consider an undirected graph  $G$  that represents  $n$  followers, which is connected, and where the leader is adjacent to at least one follower. The Laplacian matrix  $L$  of this graph is symmetric, and the matrix  $L + H$  is both positive definite and symmetric, where  $H = \text{diag} [a_{10}, a_{20}, \dots, a_{n0}]$ , where  $a_{i0}$  denotes the weight between the leader and  $i$ th agent.

### *Lemma 2* (Lai *et al.* 2024)

For  $0 < \omega \leq 1$ , it has  $(\sum_{a=1}^{\sigma} |s_i|)^{\omega} \leq \sum_{a=1}^{\sigma} |s_i|^{\omega} \leq \sigma^{1-\omega} (\sum_{a=1}^{\sigma} |s_i|)$ , where  $s_i \in \mathbb{R}$ .

**Lemma 3** (Wang *et al.* 2017)

Consider the system  $\dot{x} = f(x)$ ,  $x \in U \subseteq \mathbb{R}^n$ , and  $U$  is an open neighborhood, including the origin.  $V(x): U \rightarrow \mathbb{R}$  is positive definite and continuously differentiable. It follows from  $\dot{V}(x) + cV(x)^\alpha \leq 0, x \in U \setminus \{0\}$  that the origin is a finite-time stable equilibrium. The finite settling time satisfies  $T \leq (V(x_0))^{1-\alpha} / c(1-\alpha)$ , where  $c > 0$  and  $0 < \alpha < 1$ .

**Lemma 4** (Moulay *et al.* 2008)

Consider the system  $\dot{x}(t) = Ax(t) + \sum_{i=0}^k B_i u(t - \tau_i)$ ,  $t \geq 0$ ,  $x(t) \in \mathbb{R}^n$ ,  $u(t) \in \mathbb{R}^m$ ,  $x(0) \in \mathbb{R}^n$ ,  $u(0) \in \mathbb{R}^m$ ,  $A \in \mathbb{R}^{n \times n}$ ,  $B_i \in \mathbb{R}^{n \times m}$ , and  $\tau_i > 0$ . By using Leibniz's formula, one has  $y(t) = x(t) + \sum_{i=0}^k L_{(A,B_i)}^{h_i} u_t$ ,  $u_t: [-\tau_i, 0] \rightarrow \mathbb{R}^m$ ,  $L_{(A,B_i)}^{h_i} u_t = \int_{-\tau_i}^0 e^{A(-h_i-s)} B_i u(t+s) ds$ . One has  $\dot{y}(t) = Ay(t) + Bu(t)$  with  $B = \sum_{i=0}^k e^{-Ah_i} B_i$ . If  $\dot{y}(t) = Ay(t) + Bu(t)$  is finite-time stabilizable by  $u(t) = k(t) f(y(t))$  with  $k(t)$  bounded,  $f: \mathbb{R}^n \rightarrow \mathbb{R}^m$  continuous such that  $f(0) = 0$  and there exists  $\alpha$  of class  $K$  such that  $\|f(y)\|_m \leq \alpha(\|y\|_n)$ , then  $y(t) = x(t) + \sum_{i=0}^k L_{(A,B_i)}^{h_i} u_t$  is finite-time stabilizable by  $u(t) = k(t) f(x(t) + \sum_{i=0}^k L_{(A,B_i)}^{h_i} u_t)$ .

**Design of finite-time event-triggered control algorithm****Definition 1**

Finite-time consensus is attained if, for any given initial conditions, there exists a finite time  $T$  such that  $\lim_{t \rightarrow T} \|r_i(t) - r_0(t)\| = 0$ ,  $\lim_{t \rightarrow T} \|v_i(t) - v_0(t)\| = 0$  and  $\|r_i(t) - r_0(t)\| = 0$ , and  $\|v_i(t) - v_0(t)\| = 0$  if  $t \geq T$  if  $t \geq T$ , where  $i = 1, 2, \dots, n$ .

Consider a continuous-time dynamics model of  $n$  agents with a leader. All agents are assumed to be moving in  $m$ -dimensional space. The dynamics is specified by:

$$\dot{r}_i(t) = v_i(t), \dot{v}_i(t) = u_i(t - \tau_i) \quad (1)$$

where  $r_p$ ,  $v_p$  and  $u_i$  are defined as elements of  $\mathbb{R}^m$ , representing the position, velocity, and control input, respectively. Additionally,  $\tau_i$  signifies the constant input delay.

The leader is labeled as 0, which is specified by:

$$\dot{r}_0(t) = v_0(t), \dot{v}_0(t) = u_0(t). \quad (2)$$

Taking into account the time-delays associated with information transfer and processing, the information received by the  $i$ -th agent regarding the leader is subject to a lag, denoted as  $\tau_i$ . As a result, at any given time  $t$ , the control input for each agent is based on the states observed at  $t - \tau_i$ . This allows all follower agents to effectively monitor the delayed information from the leader. As demonstrated in Artstein (1982) and Zhou *et al.* (2025), state tracking errors are defined as  $\varepsilon_{ri} = r_i(t) - r_0(t - \tau_i)$ ,  $\varepsilon_{vi} = v_i(t) - v_0(t - \tau_i)$ . Subsequently, Artstein's transformation are applied to convert the time-delay system described by Eqs. 1 and 2 into a system devoid of delays:

$$\begin{cases} y_{1i} = \varepsilon_{ri} + \int_{-\tau_i}^0 (-\tau_i - s)(u_i(t+s) - u_0(t+s)) ds \\ y_{2i} = \varepsilon_{vi} + \int_{-\tau_i}^0 (u_i(t+s) - u_0(t+s)) ds \end{cases} \quad (3)$$

Define  $p_i = y_{1i} + \tau_i y_{2i}$ ,  $q_i = y_{2i}$  it follows that:

$$\begin{cases} \dot{p}_i = q_i \\ \dot{q}_i = u_i(t) - u_0(t) \end{cases} \quad (4)$$



To enhance the practicality of the algorithm, a distributed finite-time observer are chosen (Zhang *et al.* 2018):

$$\begin{aligned} \dot{\hat{p}}_i = & \frac{\sum_{j=0}^n a_{ij} \hat{p}_j}{\sum_{j=0}^n a_{ij}} - \frac{\alpha}{\sum_{j=0}^n a_{ij}} \text{sig}(\sum_{j=0}^n a_{ij} (\hat{p}_i - \hat{p}_j))^u \\ & - \frac{\beta}{\sum_{j=0}^n a_{ij}} \text{sig}(\sum_{j=0}^n a_{ij} (\hat{p}_i - \hat{p}_j))^v \end{aligned} \quad (5)$$

where  $\alpha, \beta > 0, 0 < u < 1, v > 1, \hat{p}_i$  is the estimate for agent  $i, \hat{p}_0 = r_0$ .

An novel finite-time consensus algorithm is developed as

$$\begin{aligned} u_i(t) = & -k_1 \text{sig}(\sum_{j=1}^n a_{ij} (p_i(t_k^i) - q_i(t_k^i)) + a_{i0} p_i(t_k^i))^{\alpha_1} \\ & - k_2 \text{sig}(\sum_{j=1}^n a_{ij} (q_i(t_k^i) - q_j(t_k^i)) + a_{i0} q_i(t_k^i))^{\alpha_2} \\ & + \ddot{\hat{p}}_i(t_k^i) \end{aligned} \quad (6)$$

where  $k_1, k_2$  denote positive constants,  $t_k^i$  is the latest event-triggered time for agent  $i, \alpha_1 \in (0, 1), \alpha_2 = \frac{2\alpha_1}{1+\alpha_1}, \text{sig}(\bullet)^{\alpha_1} = |\bullet|^{\alpha_1} \text{sgn}(\bullet), \text{sgn}(\bullet)$  is the signum function.

Define the combinational measurement state  $e_i = \sum_{j=1}^n a_{ij} (p_i - p_j) + a_{i0} p_i, g_i = \sum_{j=1}^n a_{ij} (q_i - q_j) + a_{i0} q_j$ . Define the measurement errors  $\varphi_i^e(t) = \text{sig}(e_i(t_k^i))^{\alpha_1} - \text{sig}(e_i(t))^{\alpha_1}, \varphi_i^g = \text{sig}(g_i(t_k^i))^{\alpha_2} - \text{sig}(g_i(t))^{\alpha_2}, \varphi_i^c = u_0(t_k^i) - u_0(t)$ .

The triggering function is given by:

$$h_i(t) = \|k_1 \varphi_i^e(t)\| + \|k_2 \varphi_i^g(t)\| + \|\varphi_i^c(t)\| - \xi k_2 \sqrt{m}^{1-\alpha_2} \|g_i(t)\|^{\alpha_2} \quad (7)$$

where  $\xi \in (0, 1)$ . The triggering events are generated by:

$$t_{k+1}^i = \inf\{t > t_k^i, h_i(t) > 0\}. \quad (8)$$

By using the control algorithm (6) for system (1), one has:

$$\begin{cases} \dot{e}_i = g_i \\ \dot{g}_i = -k_1 (\sum_{j=1}^n a_{ij} (\text{sig}(e_i)^{\alpha_1} - \text{sig}(e_j)^{\alpha_1}) + a_{i0} \text{sig}(e_i)^{\alpha_1}) \\ \quad - k_2 (\sum_{j=1}^n a_{ij} (\text{sig}(g_i)^{\alpha_2} - \text{sig}(g_j)^{\alpha_2}) + a_{i0} \text{sig}(g_i)^{\alpha_2}) \\ \quad - k_1 (\sum_{j=1}^n a_{ij} (\varphi_i^e - \varphi_j^e) + a_{i0} \varphi_i^e) - k_2 (\sum_{j=1}^n a_{ij} (\varphi_i^g - \varphi_j^g) + a_{i0} \varphi_i^g) \\ \quad + \sum_{j=1}^n a_{ij} (\varphi_i^c - \varphi_j^c) + a_{i0} \varphi_i^c \end{cases} \quad (9)$$

### Theorem 1

Consider the multi-agent system (1) with connected graph and the leader is a neighbor of at least one follower.

If  $\xi < 1 / \sqrt{m^{1-\alpha_2}}, k_1 > 2^{\frac{2(1+\alpha_1)}{3+\alpha_1}} \left( \frac{\rho(1+\alpha_1)\sqrt{2\lambda_{\max}}^{1+\alpha_1}}{(3+\alpha_1)\lambda_{\min}} \right), \frac{\rho}{\lambda_{\min}} < k_2 (1 - \xi \sqrt{m^{1-\alpha_2}}) \frac{3+\alpha_1}{2(1+\alpha_1)} \left( \frac{1}{2\lambda_{\min}} \right)^{\frac{1-\alpha_1}{2(1+\alpha_1)}} + k_2 \rho \sqrt{mn}^{3-\alpha_2} \left( 1 + \frac{\xi}{m} \right)^{\frac{1+\alpha_1}{\alpha_1}}$  then the event-triggered algorithm (6) solves the finite-time consensus problem under the triggering function (7).

**Proof.** The proof process is divided into three parts: 1) proving that the system is asymptotically stable; 2) constructing a new Lyapunov function to prove finite-time stability and estimating the stability time; 3) using Artstein's transformation to prove that the delayed system is finite-time stable.

Choose the Lyapunov function

$$V_1 = \frac{k_1 \sum_{i=1}^n \sum_{l=1}^m |e_{il}|^{\alpha_1+1}}{\alpha_1+1} + \frac{G^T((L+H)^{-1} \otimes I_m)G}{2} \quad (10)$$

where  $G = [g_1^T, g_2^T, \dots, g_n^T]^T$ . It follows that:

$$\begin{aligned}
\dot{V}_1(t) &= k_1 \sum_{i=1}^n \dot{e}_i^T \operatorname{sig}(e_i)^{\alpha_1} + G^T((L+H)^{-1} \otimes I_m) \dot{G} \\
&= \sum_{i=1}^n g_i^T \varphi_i^c - k_2 \sum_{i=1}^n \sum_{l=1}^m |g_{il}|^{\alpha_2+1} - k_1 \sum_{i=1}^n g_i^T \varphi_i^e - k_2 \sum_{i=1}^n g_i^T \varphi_i^g \\
&\leq -k_2 \sum_{i=1}^n \|g_i\|^{\alpha_2+1} + \sum_{i=1}^n \|g_i\| (\|k_1 \varphi_i^e\| + \|k_2 \varphi_i^g\| + \|\varphi_i^c\|) \\
&\leq -k_2 \sum_{i=1}^n \|g_i\|^{\alpha_2+1} + \xi k_2 m^{\frac{1-\alpha_2}{2}} \sum_{i=1}^n \|g_i\|^{\alpha_2+1} \\
&= -k_2 (1 - \xi \sqrt{m^{1-\alpha_2}}) \sum_{i=1}^n \|g_i\|^{\alpha_2+1}
\end{aligned} \tag{11}$$

It follows  $\xi < \frac{\sqrt{3^{1-\alpha_2}}}{\sqrt{m^{1-\alpha_2}}}$  that  $\dot{V}_1(t) \leq 0$  and  $V_1(t)$  is non-increasing. According to LaSalle's invariance theorem, it can be concluded that as  $t \rightarrow \infty$ ,  $(E^T, G^T)^T$  will converge to the set  $\{(E^T, G^T)^T | \dot{V}_1(t) \equiv 0\}$ . Clearly, the system (9) is globally asymptotically stable.

Next, the stability of  $(0_{mn}^T, 0_{mn}^T)^T$  as a finite-time-stable equilibrium will be proven. According to the findings presented in Zhao *et al.* (2016), a Lyapunov function has been developed to estimate the stability time:

$$V_2(t) = V_1(t)^{\frac{3+\alpha_1}{2(1+\alpha_1)}} + \rho E^T((L+H)^{-1} \otimes I_m)G \tag{12}$$

Young's inequality: if  $\frac{1}{x_1} + \frac{1}{x_2} = 1$ , then  $\delta_1 \delta_2 \leq c x_1 \frac{\delta_1^{x_1}}{x_1} + c^{-x_2} \frac{\delta_2^{x_2}}{x_2}$ ,  $x_1 > 1, x_2 > 1, c, \delta_1, \delta_2$  are positive. It follows Young's inequality that:

$$\begin{aligned}
&\rho E^T((L+H)^{-1} \otimes I_m)G \\
&\geq -\rho \lambda_{\max}((L+H)^{-1}) \|E\| \|G\| \\
&\geq -\frac{\rho}{\lambda_{\min}} \left( \frac{2}{3+\alpha_1} c^{\frac{3+\alpha_1}{2}} \|E\|^{\frac{3+\alpha_1}{2}} + \frac{1+\alpha_1}{3+\alpha_1} c^{-\frac{3+\alpha_1}{1+\alpha_1}} \|G\|^{\frac{3+\alpha_1}{1+\alpha_1}} \right)
\end{aligned} \tag{13}$$

$$\begin{aligned}
V_1(t)^{\frac{3+\alpha_1}{2(1+\alpha_1)}} &\geq \left( \frac{k_1}{\alpha_1+1} \sum_{i=1}^n \sum_{l=1}^m |e_{il}|^{\alpha_1+1} \right)^{\frac{3+\alpha_1}{2(1+\alpha_1)}} + \left( \frac{1}{2\lambda_{\max}} \right)^{\frac{3+\alpha_1}{2(1+\alpha_1)}} \|G\|^{\frac{3+\alpha_1}{1+\alpha_1}} \\
&\leq 2^{\frac{1-\alpha_1}{2(1+\alpha_1)}} \left( \frac{k_1 \sqrt{3n}^{1-\alpha_1}}{\alpha_1+1} \right)^{\frac{3+\alpha_1}{2(1+\alpha_1)}} \|E\|^{\frac{3+\alpha_1}{2}} + \frac{1}{2} \left( \frac{1}{\lambda_{\min}} \right)^{\frac{3+\alpha_1}{2(1+\alpha_1)}} \|G\|^{\frac{3+\alpha_1}{1+\alpha_1}}
\end{aligned} \tag{14}$$

where  $\lambda_{\max}, \lambda_{\min}$  denotes the maximum and minimum eigenvalues of  $L+H$ , respectively.

Substituting (13) and (14) into Eq. 12 yields:

$$\begin{aligned}
V_2(t) &\geq \left( \left( \frac{k_1}{\alpha_1+1} \right)^{\frac{3+\alpha_1}{2(1+\alpha_1)}} - \frac{2\rho c^{\frac{3+\alpha_1}{2}}}{(3+\alpha_1)\lambda_{\min}} \right) \|E\|^{\frac{3+\alpha_1}{2}} \\
&\quad + \left( \left( \frac{1}{2\lambda_{\max}} \right)^{\frac{3+\alpha_1}{2(1+\alpha_1)}} - \frac{\rho(1+\alpha_1)c^{-\frac{3+\alpha_1}{1+\alpha_1}}}{(3+\alpha_1)\lambda_{\min}} \right) \|G\|^{\frac{3+\alpha_1}{1+\alpha_1}}
\end{aligned} \tag{15}$$

If  $c$  is in the interval  $\sqrt{2\lambda_{\max}} \left( \frac{(\alpha_1+1)\rho}{(3+\alpha_1)\lambda_{\min}} \right) < c < \left( \frac{(3+\alpha_1)\lambda_{\min}}{2\rho} \right)^{\frac{2}{3+\alpha_1}} \left( \frac{k_1}{\alpha_1+1} \right)^{\frac{1}{\alpha_1+1}}$ , then we have  $V_2(t)$  is radially unbounded and positive definite. Set  $c = v \sqrt{2\lambda_{\max}} \left( \frac{(\alpha_1+1)\rho}{(3+\alpha_1)\lambda_{\min}} \right) + (1-v) \left( \frac{(3+\alpha_1)\lambda_{\min}}{2\rho} \right)^{\frac{2}{3+\alpha_1}} \left( \frac{k_1}{\alpha_1+1} \right)^{\frac{1}{\alpha_1+1}}$ ,  $0 < v < 1, k_1 > 2^{\frac{2(1+\alpha_1)}{3+\alpha_1}} \left( \frac{\rho(1+\alpha_1)\sqrt{2\lambda_{\max}}}{(3+\alpha_1)\lambda_{\min}} \right)^{1+\alpha_1}$  then  $V_2(t)$  is an effective Lyapunov function.



Similarly, based on Young's inequality, we can obtain:

$$\begin{aligned} \rho E^T ((L + H)^{-1} \otimes I_m) G &\leq \frac{\rho}{\lambda_{\min}} \|E\| \|G\| \\ &\leq \frac{\rho}{\lambda_{\min}} \left( \frac{2}{3+\alpha_1} c^{\frac{3+\alpha_1}{2}} \|E\|^{\frac{3+\alpha_1}{2}} + \frac{1+\alpha_1}{3+\alpha_1} c^{\frac{3+\alpha_1}{1+\alpha_1}} \|G\|^{\frac{3+\alpha_1}{1+\alpha_1}} \right) \end{aligned} \quad (16)$$

$$\begin{aligned} V_1(t)^{\frac{3+\alpha_1}{2(1+\alpha_1)}} &\leq 2^{\frac{1-\alpha_1}{2(1+\alpha_1)}} \left( \frac{k_1}{\alpha_1+1} \sum_{i=1}^n \sum_{l=1}^m |e_{il}|^{\alpha_1+1} \right)^{\frac{3+\alpha_1}{2(1+\alpha_1)}} + \frac{1}{2} \left( \frac{1}{\lambda_{\min}} \right)^{\frac{3+\alpha_1}{2(1+\alpha_1)}} \|G\|^{\frac{3+\alpha_1}{1+\alpha_1}} \\ &\leq 2^{\frac{1-\alpha_1}{2(1+\alpha_1)}} \left( \frac{k_1 \sqrt{3n}^{1-\alpha_1}}{\alpha_1+1} \right)^{\frac{3+\alpha_1}{2(1+\alpha_1)}} \|E\|^{\frac{3+\alpha_1}{2}} + \frac{1}{2} \left( \frac{1}{\lambda_{\min}} \right)^{\frac{3+\alpha_1}{2(1+\alpha_1)}} \|G\|^{\frac{3+\alpha_1}{1+\alpha_1}} \end{aligned} \quad (17)$$

Furthermore, one has:

$$\begin{aligned} V_2 &\leq \left( \frac{\rho}{\lambda_{\min}} \frac{1+\alpha_1}{3+\alpha_1} c^{\frac{3+\alpha_1}{1+\alpha_1}} + \frac{1}{2} \left( \frac{1}{\lambda_{\min}} \right)^{\frac{3+\alpha_1}{2(1+\alpha_1)}} \right) \|G\|^{\frac{3+\alpha_1}{1+\alpha_1}} \\ &\quad + \left( \frac{2\rho c^{\frac{3+\alpha_1}{2}}}{\lambda_{\min}(3+\alpha_1)} + 2^{\frac{1-\alpha_1}{2(1+\alpha_1)}} \left( \frac{k_1 \sqrt{3n}^{1-\alpha_1}}{\alpha_1+1} \right)^{\frac{3+\alpha_1}{2(1+\alpha_1)}} \right) \|E\|^{\frac{3+\alpha_1}{2}} \\ &= \varpi_1 \|E\|^{\frac{3+\alpha_1}{2}} + \varpi_2 \|G\|^{\frac{3+\alpha_1}{1+\alpha_1}} \end{aligned} \quad (18)$$

where  $\varpi_1 = \frac{\rho}{\lambda_{\min}} \frac{2}{3+\alpha_1} c^{\frac{3+\alpha_1}{2}} + 2^{\frac{1-\alpha_1}{2(1+\alpha_1)}} \left( \frac{k_1 \sqrt{3n}^{1-\alpha_1}}{\alpha_1+1} \right)^{\frac{3+\alpha_1}{2(1+\alpha_1)}}$ ,  $\varpi_2 = \frac{\rho}{\lambda_{\min}} \frac{1+\alpha_1}{3+\alpha_1} c^{\frac{3+\alpha_1}{1+\alpha_1}} + \frac{1}{2} \left( \frac{1}{\lambda_{\min}} \right)^{\frac{3+\alpha_1}{2(1+\alpha_1)}}$ .

Taking the derivative of  $V_2(t)$  yields:

$$\begin{aligned} \dot{V}_2(t) &\leq -k_2 \left( 1 - \xi \sqrt{m^{1-\alpha_2}} \right) \frac{3+\alpha_1}{2(1+\alpha_1)} \left( \frac{1}{2\lambda_{\min}} \right)^{\frac{1-\alpha_1}{2(1+\alpha_1)}} \|G\|^2 + \frac{\rho}{\lambda_{\min}} \|G\|^2 \\ &\quad - k_1 \rho \|E\|^{\alpha_1+1} + k_2 \rho \sqrt{mn}^{3-\alpha_2} \|E\| \|G\|^{\alpha_2} + k_2 \rho \xi \sqrt{3}^{1-\alpha_2} \sqrt{n}^{3-\alpha_2} \|E\| \|G\|^{\alpha_2} \\ &\leq -\rho \left( k_1 - k_2 \sqrt{3n}^{3-\alpha_2} \left( 1 + \frac{\xi}{m} \right) \frac{\alpha_1 c^{\frac{1+\alpha_1}{\alpha_1}}}{1+\alpha_1} \right) \|E\|^{\alpha_1+1} \\ &\quad - \left( k_2 \left( 1 - \xi \sqrt{3^{1-\alpha_2}} \right) \frac{3+\alpha_1}{2(1+\alpha_1)} \left( \frac{1}{2\lambda_{\min}} \right)^{\frac{1-\alpha_1}{2(1+\alpha_1)}} \right) \|G\|^2 \\ &\quad + \left( \frac{\rho}{\lambda_{\min}} + k_2 \rho \sqrt{3n}^{3-\alpha_2} \left( 1 + \frac{\xi}{m} \right) \frac{\alpha_1 c^{\frac{1+\alpha_1}{\alpha_1}}}{1+\alpha_1} \right) \|G\|^2 = -l_1 \|E\|^{\alpha_1+1} - l_2 \|G\| \\ &\leq - \left( l_1^{\frac{3+\alpha_1}{2(1+\alpha_1)}} \|E\|^{\frac{3+\alpha_1}{2}} + l_2^{\frac{3+\alpha_1}{2(1+\alpha_1)}} \|G\|^{\frac{3+\alpha_1}{1+\alpha_1}} \right)^{\frac{2(1+\alpha_1)}{3+\alpha_1}} \leq -l_3 V_2(t)^{\frac{2(1+\alpha_1)}{3+\alpha_1}} \end{aligned} \quad (19)$$

where  $l_1^{\frac{3+\alpha_1}{2(1+\alpha_1)}} - l_3^{\frac{3+\alpha_1}{2(1+\alpha_1)}} \varpi_1 > 0$ ,  $l_1^{\frac{3+\alpha_1}{2(1+\alpha_1)}} - l_3^{\frac{3+\alpha_1}{2(1+\alpha_1)}} \varpi_1 > 0$ ,

$$l_1 = k_1 - k_2 \sqrt{3n}^{3-\alpha_2} \left( 1 + \frac{\xi}{m} \right) \frac{\alpha_1 c^{\frac{1+\alpha_1}{\alpha_1}}}{1+\alpha_1},$$

$$l_2 = k_2 \left( 1 - \xi \sqrt{3^{1-\alpha_2}} \right) \frac{3+\alpha_1}{2(1+\alpha_1)} \left( \frac{1}{2\lambda_{\min}} \right)^{\frac{1-\alpha_1}{2(1+\alpha_1)}} - \frac{\rho}{\lambda_{\min}} - k_2 \rho \sqrt{3n}^{3-\alpha_2} \left( 1 + \frac{\xi}{m} \right) \frac{\alpha_1 c^{\frac{1+\alpha_1}{\alpha_1}}}{1+\alpha_1}.$$

It follows from Lemma 3 that the system (9) can be stabilized within a finite time, with the upper bound for the stability time being:

$$t \leq T_1 = \frac{3+\alpha_1}{\gamma_3(1-\alpha_1)} V_2(0)^{\frac{1-\alpha_1}{3+\alpha_1}} \quad (20)$$

From the combinational state  $e_p, g_p$  we get  $p_i = y_{1i} + \tau_i y_{2i} = 0_m, q_i = y_{2i} = 0_{1-d_1^i}, t > T_1 = \frac{3+\alpha_1}{\gamma_3(1-\alpha_1)} V_2(0)^{\frac{1-\alpha_1}{3+\alpha_1}}$ . Furthermore,  $\int_{-\tau_i}^0 (u_i(t+s) - u_0(t+s)) ds$  converges to 0 with settling time  $\frac{3+\alpha_1}{\gamma_3(1-\alpha_1)} V_2(0)^{\frac{1-\alpha_1}{3+\alpha_1}} + \max\{\tau_i\}$ . The time-delay system (1) (2) is finite-time stable. This completes the proof.

The following theorem proves that the Zeno triggering does not exist.

### Theorem 2

Consider a time-delay system (1) and (2), in accordance with the stipulations outlined in Theorem 1. Then, for any time  $t \geq 0$ , agent  $i$  will avoid the Zeno behavior before consensus is achieved.

Proof. For  $t \in [t_k^i, t_{k+1}^i)$ , we have:

$$\begin{aligned} \|k_1 \varphi_i^e\| &= k_1 \left\| \text{sig}(e_i(t_k^i))^{\alpha_1} - \text{sig}(e_i(t))^{\alpha_1} \right\| \leq k_1 2^{1-\alpha_1} 3^{\frac{1-\alpha_1}{2}} \|e_i(t_k^i) - e_i(t)\|^{\alpha_1} \\ &= k_1 2^{1-\alpha_1} 3^{\frac{1-\alpha_1}{2}} \left\| \int_{t_k^i}^t g_i(\tau) d\tau \right\|^{\alpha_1} \leq k_1 2^{1-\alpha_1} 3^{\frac{1-\alpha_1}{2}} \|g_i(t)\|^{\alpha_1} (t - t_k^i)^{\alpha_1} \end{aligned} \quad (21)$$

Similarly, we can obtain:

$$\|k_2 \varphi_i^g\| = k_2 2^{1-\alpha_2} 3^{\frac{1-\alpha_2}{2}} \|g_i(t)\|^{\alpha_2} (t - t_k^i)^{\alpha_2} \|\dot{\tilde{p}}_i\| \leq \left\| \frac{d}{dt} \tilde{p}_i \right\| (t - t_k^i) \quad (22)$$

Define  $\vartheta_1 = \max\{2^{1-\alpha_1} 3^{\frac{1-\alpha_1}{2}} \|g_i(t)\|^{\alpha_1}, k_2 2^{1-\alpha_2} 3^{\frac{1-\alpha_2}{2}} \|g_i(t)\|^{\alpha_2}, \left\| \frac{d}{dt} \tilde{p}_i \right\|\}$ , one can obtain that:

$$\begin{aligned} \vartheta_1 \left( (t_{k+1}^i - t_k^i)^{\alpha_1} + (t_{k+1}^i - t_k^i)^{\alpha_2} + (t_{k+1}^i - t_k^i) \right) &\geq 2^{1-\alpha_1} 3^{\frac{1-\alpha_1}{2}} \|g_i(t)\|^{\alpha_1} (t_{k+1}^i - t_k^i)^{\alpha_1} \\ + \left\| \frac{d}{dt} \tilde{p}_i \right\| (t_{k+1}^i - t_k^i) + k_2 2^{1-\alpha_2} 3^{\frac{1-\alpha_2}{2}} \|g_i(t)\|^{\alpha_2} (t_{k+1}^i - t_k^i)^{\alpha_2} &\geq k_2 \xi 3^{\frac{1-\alpha_2}{2}} \|g_i(t)\|^{\alpha_2} \end{aligned} \quad (23)$$

Then, we have:

$$(t_{k+1}^i - t_k^i) > 0. \quad (24)$$

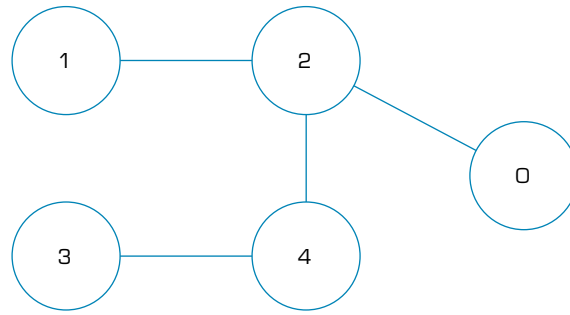
We can conclude that time-delay system does not exhibit Zeno behavior before consensus is achieved. This completes the proof.

In practical scenarios, the topology may undergo changes as a result of factors such as communication distance, physical device malfunctions, or other contributing circumstances. To tackle this problem, switching topologies  $G = \{G_o \mid o = 1, 2, \dots, c\}$ ,  $c \in \mathbb{N}^+$ .  $\sigma(t): [0, +\infty) \rightarrow k$  denoting switching signal were introduced. Without loss of generality,  $G$  is time invariant for  $[t_k^i, t_{k+1}^i)$ . Next, the results on switching topologies are given.

**Corollary 1** – Assume that each topology is connected and the leader is a neighbor of at least one follower. If  $\xi < 1 / \sqrt{m^{1-\alpha_2}}$ ,  $k_1 > 2^{\frac{2(1+\alpha_1)}{3+\alpha_1}} \left( \frac{\rho(1+\alpha_1)\sqrt{2\lambda_{\max}}^{1+\alpha_1}}{(3+\alpha_1)\lambda_{\min}} \right)$ ,  $\xi \sqrt{m^{1-\alpha_2}} \frac{3+\alpha_1}{2(1+\alpha_1)} \left( \frac{1}{2\lambda_{\min}} \right)^{\frac{1-\alpha_1}{2(1+\alpha_1)}} + k_2 \rho \sqrt{mn}^{3-\alpha_2} \left( 1 + \frac{\xi}{m} \right)^{\frac{\alpha_1 c}{1+\alpha_1}}$ , then the event-triggered algorithm (6) solves the finite-time consensus problem of time-delay multi-agent system (1) (2) under the triggering function (7).

**Example 1:** to assess the efficacy of the proposed algorithm, a numerical simulation are presented. The topology is shown in Fig. 1. All agents are assumed to be moving in 1-dimensional space.

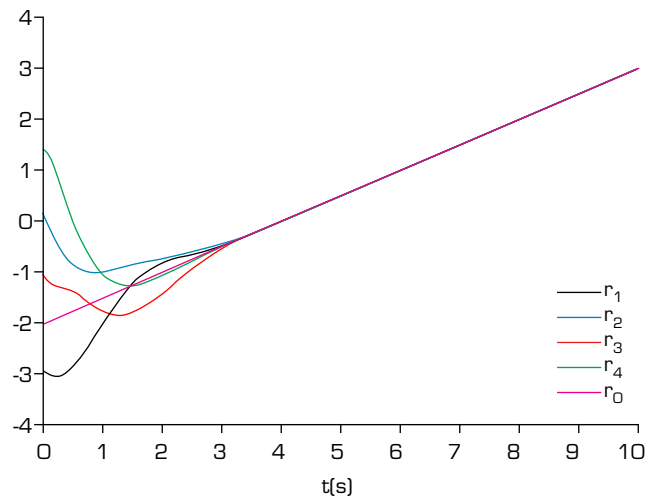




Source: Elaborated by the authors.

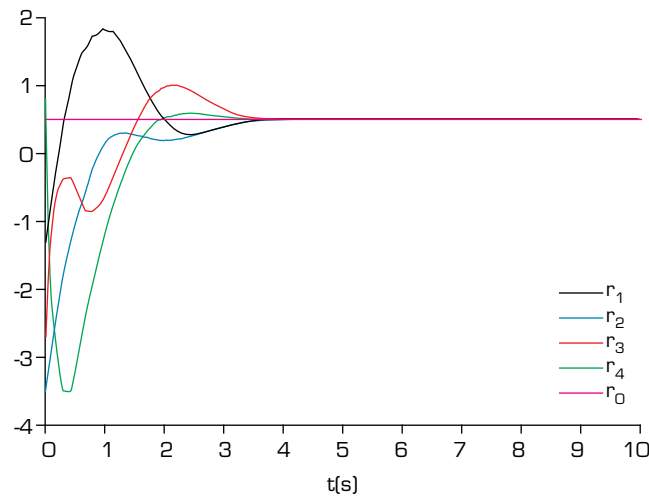
**Figure 1.** The undirected communication topology.

We choose  $\alpha_1 = 0.5$ ,  $k_1 = 6$ ,  $k_2 = 5.5$ ,  $\xi = 0.25$ ,  $\tau_i = 0.1$ . The initial positions and velocities are randomly generated in the interval  $[-5, 5]$ . With the event-triggered algorithm (3) and triggering function (4), the trajectories are shown in Figs. 2 and 3. The measurement errors  $\|k_1 \varphi_i^e(t)\| + \|k_2 \varphi_i^g(t)\| + \|\varphi_i^e(t)\|$  and thresholds  $\xi k_2 \sqrt{m}^{1-\alpha_2} \|g_i(t)\|^{\alpha_2}$  are shown in Fig. 4.



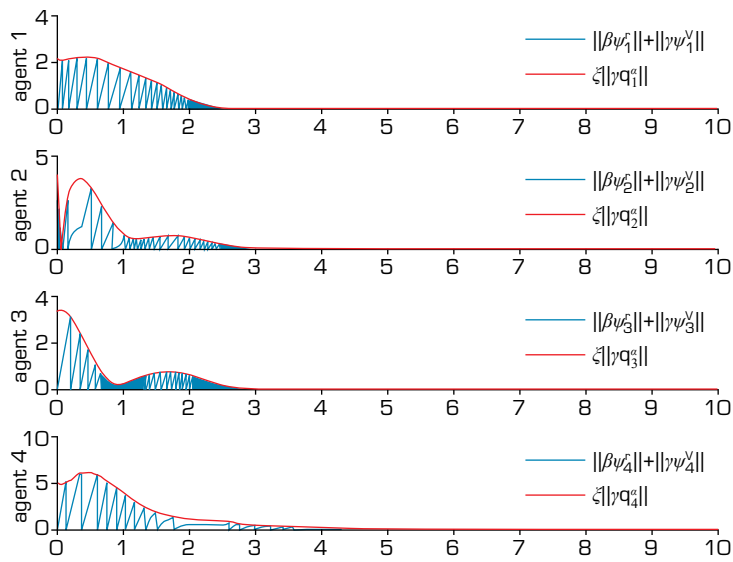
Source: Elaborated by the authors.

**Figure 2.** Position trajectory.



Source: Elaborated by the authors.

**Figure 3.** Velocity trajectory.



Source: Elaborated by the authors.

**Figure 4.** Combinational measurement errors and thresholds.

Figures 2 and 3 show that consensus is achieved in finite time. The combinational measurement errors and thresholds indicate the asynchronous event sequences from Fig. 4. When an agent is triggered at its triggering time, its measurement error is set to 0 due to the status update. Each agent’s controller only updates at its triggering time, reducing energy consumption.

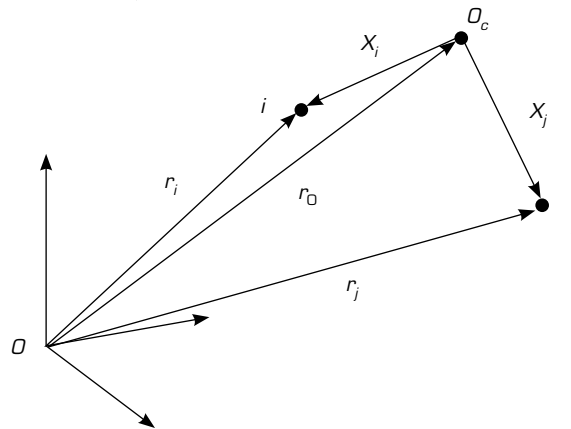
### Design of finite-time formation control algorithm

Before proceeding, the definition of finite-time formation control is first provided.

#### Definition 2

The finite-time formation control problem is considered resolved when the states of the agents meet specific criteria:  $\lim_{t \rightarrow T} \|r_i(t) - x_i - r_0(t)\| = 0$ ,  $\lim_{t \rightarrow T} \|v_i(t)\| = \|v_0(t)\|$  and  $\|r_i(t) - x_i - r_0(t)\| = 0$ ,  $\|v_i(t)\| = \|v_0(t)\|$  when  $t \geq T$ . Where  $T$  denotes a finite time,  $x_i$  denotes the position vector between agent  $i$  and leader,  $i = 1, 2, \dots, n$ .

For convenience, a model transformation is performed for comprehension. A Cartesian coordinate is shown in Fig. 5, where  $r_0$  is the position of formation center and is represented by  $O_c$ ,  $O$  is the origin,  $r_i$  denote the positions of agent  $i, j$ , respectively. The position vector between agent  $i$  and leader is  $x_i$ . Then, we can transform  $\lim_{t \rightarrow T} \|r_i(t) - r_j(t) - x_{ij}\| = 0$  into  $\lim_{t \rightarrow T} \|(r_i(t) - x_i) - (r_j(t) - x_j)\| = 0$ , where  $x_{ij} = x_i - x_j$ .



Source: Elaborated by the authors.

**Figure 5.** Cartesian coordinate.



From Artstein's transformation (3) (4), a distributed finite-time formation control algorithm is defined as

$$u_i = -k_1 \text{sig} \left( \sum_{j=1}^N a_{ij} \left( (p_i(t_k^i) - p_j(t_k^i) - x_{ij}) + a_{i0}(p_i(t_k^i) - x_i) \right)^{\alpha_1} \right. \\ \left. - k_2 \text{sig} \left( \sum_{j=1}^N a_{ij} \left( q_i(t_k^i) - q_j(t_k^i) \right) + a_{i0} q_i(t_k^i) \right)^{\alpha_2} \right) + \ddot{p}_i(t_k^i) \quad (25)$$

where  $x_{ij} \in R^3$  is the expect position between agent  $i$  and  $j$ ,  $x_i \in R^3$  is the expect position between agent  $i$  and the leader,  $x_{ij} = x_i - x_j$ .

Similarly, define  $e_i = \sum_{j=1}^N a_{ij}(p_i - p_j - x_{ij}) + a_{i0}(p_i - x_i)$ ,  $g_i = \sum_{j=1}^N a_{ij}(q_i - q_j) + a_{i0}q_i$ . Define the measurement errors  $\varphi_i^e = \text{sig} \left( e_i(t_k^i) \right)^{\alpha_1} - \text{sig} \left( e_i(t) \right)^{\alpha_1}$ ,  $\varphi_i^g = \text{sig} \left( g_i(t_k^i) \right)^{\alpha_2} - \text{sig} \left( g_i(t) \right)^{\alpha_2}$ ,  $\varphi_i^c = u_0(t_k^i) - u_0(t)$ . The triggering function is given by

$$h_i(t) = \|\beta \varphi_i^e(t)\| + \|\gamma \varphi_i^g(t)\| + \|\varphi_i^c(t)\| - \xi \gamma 3^{\frac{1-\alpha_2}{2}} \|\dot{g}_i\|^{\alpha_2} \quad (26)$$

### Theorem 3

Consider the time-delay system (1) (2) with connected graph and the leader is a neighbor of at least one agent. If  $\xi < 1/\sqrt{3^{1-\alpha_2}}$ ,  $k_1 > 2^{\frac{2(1+\alpha_1)}{3+\alpha_1}} \left( \frac{\rho(1+\alpha_1)\sqrt{2\lambda_{\max}}}{(3+\alpha_1)\lambda_{\min}} \right)^{1+\alpha_1} k_2 (1 - \xi \sqrt{m^{1-\alpha_2}})^{\frac{3+\alpha_1}{2(1+\alpha_1)}} \left( \frac{1}{2\lambda_{\min}} \right)^{\frac{1-\alpha_1}{2(1+\alpha_1)}} + k_2 \rho \sqrt{mn}^{3-\alpha_2} \left( 1 + \frac{\xi}{m} \right)^{\frac{\alpha_1 c}{1+\alpha_1}}$ , then the event-triggered algorithm (25) solves the finite-time formation control problem under the triggering function (26).

Proof. We first prove that  $\hat{p}_i \rightarrow p_0$ ,  $i = 1, 2, \dots, n$ , in finite time. Define  $\phi_i = \sum_{j=1}^n a_{ij}(\hat{p}_i - \hat{p}_j) + a_{i0}(\hat{p}_i - p_0)$ , it follows from (5) that:

$$\dot{\phi}_i = -\eta \text{sig}(\phi_i)^{\alpha_1} \quad (27)$$

Choose the Lyapunov function candidate,  $V_3(t) = \frac{1}{2} \phi^T \phi$ , where  $\phi = (\phi_1^T, \phi_2^T, \dots, \phi_n^T)^T$ . One has:

$$\dot{V}_3(t) = -\eta \sum_{i=1}^n \phi_i^T \text{sig}(\phi_i)^{\alpha_1} = -\eta \sum_{i=1}^n \sum_{j=1}^n |\phi_{ij}|^{\alpha_1+1} \\ \leq -\eta \|\phi\|^{\alpha_1+1} = -\eta 2^{\frac{\alpha_1+1}{2}} V_3^{\frac{\alpha_1+1}{2}}(t). \quad (28)$$

From Lemma 3, there exists a finite time  $T_2 \leq \frac{(2V_3(0))^{\frac{1-\alpha_1}{2}}}{\eta}$ , such that  $\|\phi\| = 0$ ,  $\forall t \geq T_2$ . Note that  $\phi = ((L + H) \otimes I_3)(\hat{p} - 1_n p_0)$ ,  $\hat{p} = (\hat{p}_1^T, \hat{p}_2^T, \dots, \hat{p}_n^T)^T$ . We can obtain that  $\|\hat{p}_i - p_0\| = 0$ ,  $\forall t \geq T_2$ .

Then, the proof is similar to Theorem 1 and is hence omitted here. This completes the proof.

Similarly Corollary 1, the control algorithm (25) can be used for switching topologies.

### Finite-time formation control for UAVs

In this section, the model of the UAV is first presented. The model is then transformed into an accurate linearized model by utilizing feedback linearization. Consider UAV systems composed of  $n$  UAVs and a leader (labeled as 0), where the leader is a neighbor of at least one UAV. The model of the UAV is defined as

$$\begin{cases} \dot{x}_i = V_i \cos \theta_i \cos \psi_i \\ \dot{y}_i = V_i \sin \theta_i \\ \dot{z}_i = -V_i \cos \theta_i \sin \psi_i \\ \dot{V}_i = g(\eta_{xi}(t - \tau_i) - \sin \theta_i) \\ \dot{\theta}_i = \frac{g}{V_i} (\eta_{yi}(t - \tau_i) - \cos \theta_i) \\ \dot{\psi}_i = -\frac{g}{V_i \cos \theta_i} \eta_{zi}(t - \tau_i) \end{cases} \quad (29)$$

where  $x_p, y_p, z_p$  represent the position within an inertial coordinate system, while  $V_i$  denotes the velocity. The flight-path angle is indicated by  $\theta_p$ , and the heading angle is represented by  $\psi_p$ . The acceleration due to gravity is denoted by  $g$ . Additionally, the components of overload along the trajectory coordinate axes are represented by  $\eta_{xi}, \eta_{yp}, \eta_{zi}$ , where the index  $i$  ranges from 0 to  $n$ .

Then, we have:

$$\dot{\varphi}_i = f(\varphi_i) + c(\varphi_i)\eta_i \quad (30)$$

$$\text{where } \varphi_i = (x_p, y_p, z_p, V_p, \theta_p, \psi_i)^T, \eta_i = (\eta_{xi}, \eta_{yp}, \eta_{zi})^T, f(\varphi_i) = \begin{bmatrix} V_i \cos \theta_i \cos \psi_i \\ V_i \sin \theta_i \\ -V_i \cos \theta_i \sin \psi_i \\ -g \sin \theta_i \\ -\frac{g}{V_i} \cos \theta_i \\ 0 \end{bmatrix}, c(\varphi_i) = \begin{bmatrix} 0 & 0 & 0 \\ 0 & 0 & 0 \\ 0 & 0 & 0 \\ g & 0 & 0 \\ 0 & \frac{g}{V_i} & 0 \\ 0 & 0 & \frac{-g}{V_i \cos \theta_i} \end{bmatrix}$$

Subsequent application of feedback linearization results in:

$$\dot{\zeta}_i = A\zeta_i + Bu_i \quad (31)$$

where  $\zeta_i = (x_p, y_p, z_p, \dot{x}_p, \dot{y}_p, \dot{z}_p)^T$ ,  $A = \begin{pmatrix} 0_{3 \times 3} & I_{3 \times 3} \\ 0_{3 \times 3} & 0_{3 \times 3} \end{pmatrix}$ ,  $B = \begin{pmatrix} 0_{3 \times 3} \\ I_{3 \times 3} \end{pmatrix}$ .

The state feedback transformation can be specified by:

$$u_i = g \begin{bmatrix} \cos \theta_i \cos \psi_i & -\sin \theta_i \cos \psi_i & \sin \psi_i \\ \sin \theta_i & \cos \theta_i & 0 \\ -\cos \theta_i \sin \psi_i & \sin \theta_i \sin \psi_i & \cos \psi_i \end{bmatrix} \begin{pmatrix} \eta_{xi} \\ \eta_{yi} \\ \eta_{zi} \end{pmatrix} - \begin{pmatrix} 0 \\ g \\ 0 \end{pmatrix} \quad (32)$$

A nonsingular smooth vector function is selected as  $r_i = (x_p, y_p, z_p)^T$ . Then, (29) can be expressed as the following delayed second-order system:

$$\ddot{r}_i = u_i(t - \tau_i) \quad (33)$$

By utilizing Theorem 3, the finite-time formation control algorithm can control multiple UAVs to maintain the formation shape.

Example 2: the switching communication topologies are shown in Fig. 6. Choose  $\alpha_1 = 0.5$ ,  $k_1 = 6$ ,  $k_2 = 5.5$ ,  $\xi = 0.25$ ,  $\tau_i = 0.1$ . The simulation time is 200 s. The leader is specified by:

$$\begin{cases} V_0 = 180 + 15 \sin(0.2t) \\ \theta_0 = 0.1 \sin(0.05t) \\ \psi_0 = 0.02 \sin(0.1t) \end{cases} \quad (34)$$

Source: Elaborated by the authors.

**Figure 6.** The switching communication topologies.

The desired formation vectors are given by  $x_1 = [-500 \ -50 \ -200]^T$ ,  $x_2 = [-500 \ -50 \ 200]^T$ ,  $x_3 = [-1000 \ -100 \ -400]^T$ ,  $x_4 = [-1000 \ -100 \ 400]^T$ .

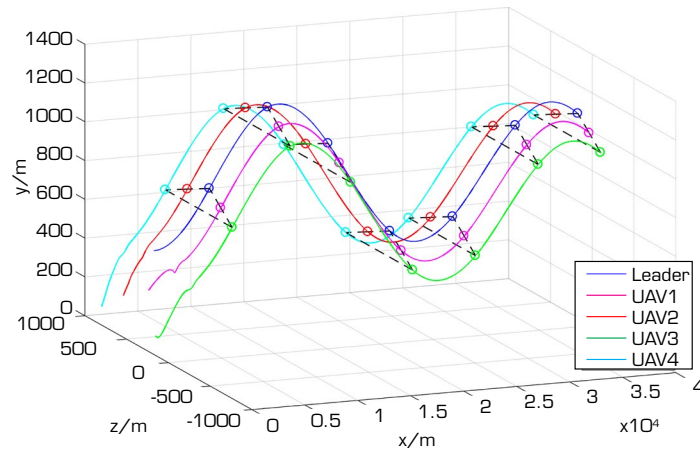
The initial conditions are established in accordance with the specifications outlined in Table 1.

**Table 1.** The initial state of multiple UAVs.

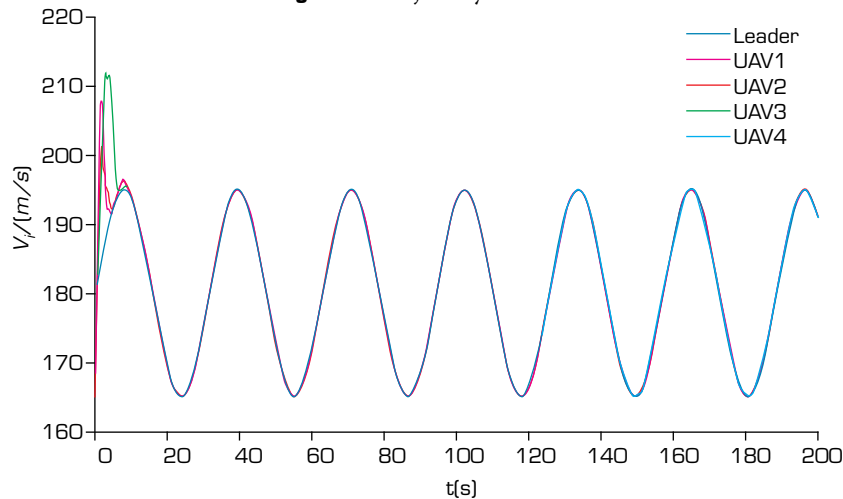
State	$x_i$ (m)	$y_i$ (m)	$z_i$ (m)	$V_i$ (m/s)	$\theta_i$ (°)	$\psi_i$ (°)
UAV1	500	300	300	170	5	9
UAV2	400	200	600	165	8	-3
UAV3	50	150	100	185	-4	5
UAV4	100	100	700	190	-6	2
Leader	1,000	500	300	180	0	0

Source: Elaborated by the authors.

The trajectories of the UAVs are illustrated in Fig. 7. This figure demonstrates that, when employing the event-triggered controller (25), all UAVs successfully follow the trajectory of the leader UAV within a finite time frame. The corresponding velocity, flight-path angle, and heading angle are depicted in Figs. 8–10, respectively. The simulation results indicate that the velocity, flight-path angle, and heading angle of all UAVs effectively align with those of the leader UAV. Additionally, all UAVs sustain the desired formation shape throughout the formation flight, thereby validating the efficacy of the proposed algorithm and the precision of the linearized model.

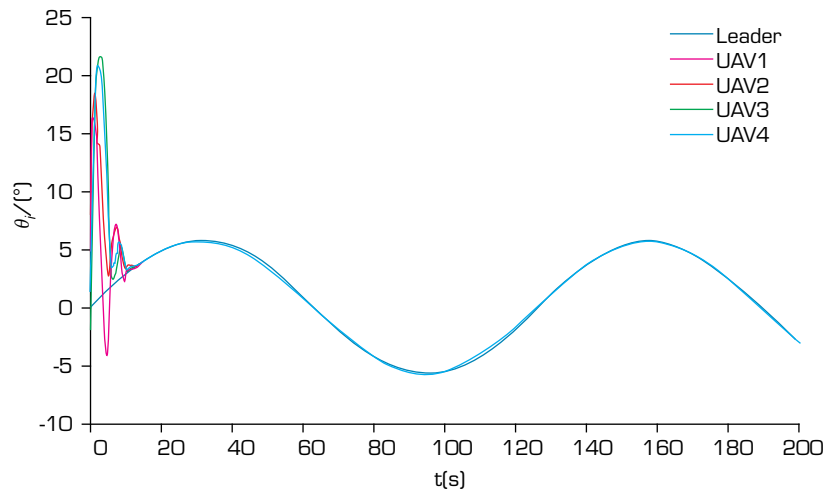


Source: Elaborated by the authors.

**Figure 7.** Trajectory of UAVs.

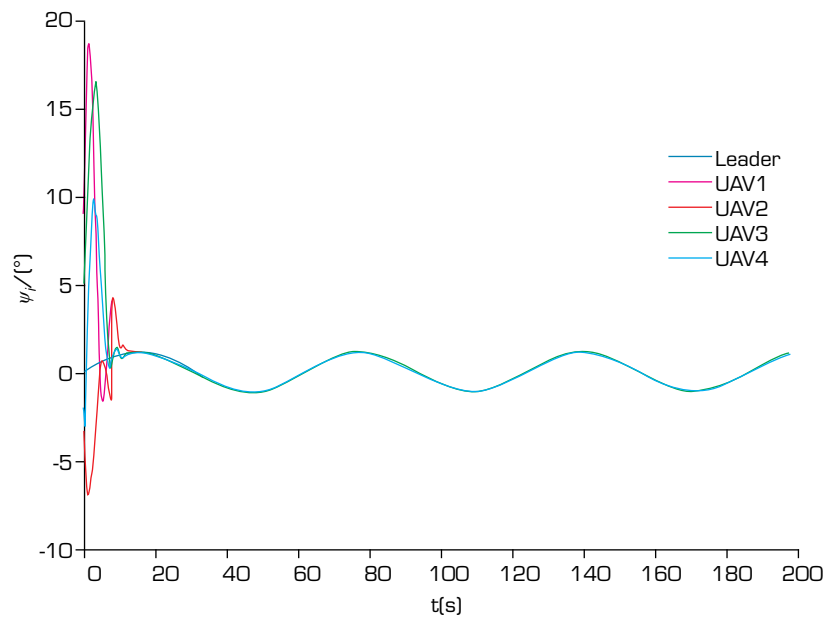
Source: Elaborated by the authors.

**Figure 8.** Velocity of UAVs.



Source: Elaborated by the authors.

**Figure 9.** Flight-path angle of UAVs.



Source: Elaborated by the authors.

**Figure 10.** Heading angle of UAVs.

## CONCLUSION

In this study, the finite-time formation control problem of second-order time-delay multi-agent systems was investigated. To reduce the frequency of controller updates, a novel finite-time control algorithm was proposed by employing event-triggered control. Using some lemmas and finite-time stability theory, theoretical analysis was performed. It was also proven that Zeno behavior does not exhibit when employing the proposed triggering function. The finite-time formation control algorithm was designed based on the finite-time consensus algorithm. Using the feedback linearization technique, the model of the UAV was transformed into an accurate linearized model. Finally, the simulation of the UAV demonstrated that the proposed formation control algorithm effectively solves the finite-time formation control problem.

## CONFLICT OF INTEREST

Nothing to declare.

## AUTHORS' CONTRIBUTION

**Conceptualization:** Zhang H; **Methodology:** Zhang H; **Analysis:** Zhou D; **Writing – Original Draft:** Zhang H and Zhou D; **Writing – Review and Editing:** Zhou D; **Final approval:** Zhou D.

## DATA AVAILABILITY STATEMENT

The data will be available upon request.

## FUNDING

The author Haini Zhang is supported by Distinguished Youth Cultivation Program of Jiangsu Vocational Institute of Commerce.

## ACKNOWLEDGEMENTS

To the editor and the reviewers, for their constructive feedback and valuable suggestions, which significantly enhanced the quality of this paper.

## REFERENCES

- Ahmed F, Mohanta J, Keshari A, Yadav PS (2022) Recent advances in unmanned aerial vehicles: a review. *Arab J Sci Eng* 47(7):7963-7984. <https://doi.org/10.1007/s13369-022-06738-0>
- Amirkhani A, Barshooi AH (2022) Consensus in multi-agent systems: a review. *Artif Intel Rev* 55(5):3897-3935. <https://doi.org/10.1007/s10462-021-10097-x>
- An S, Liu Y, Wang X, Fan Z, Zhang Q, He Y, Wang L (2023) Distributed event-triggered fixed-time leader-follower formation tracking control of multiple underwater vehicles based on an adaptive fixed-time observer. *J Mar Sci Eng* 11(8):522. <https://doi.org/10.3390/jmse11081522>
- Artstein Z (1982) Linear systems with delayed controls: a reduction. *IEEE Trans Autom Control* 27(4):869-879. <https://doi.org/10.1109/TAC.1982.1103023>
- Dou L, Cai S, Zhang X, Su X, Zhang R (2022) Event-triggered based adaptive dynamic programming for distributed formation control of multi-uav. *J Frank Inst* 359(8):3671-3691. <https://doi.org/10.1016/j.jfranklin.2022.02.034>
- Gargalakos M (2024) The role of unmanned aerial vehicles in military communications: application scenarios, current trends, and beyond. *J Def Model Simul* 21(3):313-321. <https://doi.org/10.1177/15485129211031668>

- Gong S, Zheng M, Hu J, Zhang A (2023) Event-triggered cooperative control for high-order nonlinear multi-agent systems with finite-time consensus. *Int J Appl Math Comput Sci* 33(3):439-448. <https://doi.org/10.34768/amcs-2023-0032>
- Hou Z, Lu P (2022) Event-triggered integral sliding mode formation control for multiple quadrotor uavs with unknown disturbances. *J Frank Inst* 1:17-29. <https://doi.org/10.1016/j.fraope.2022.05.004>
- Huang B, Song S, Zhu C, Li J, Zhou B (2021) Finite-time distributed formation control for multiple unmanned surface vehicles with input saturation. *Ocean Eng* 233:109158. <https://doi.org/10.1016/j.oceaneng.2021.109158>
- Huang C, Zhang X, Zhang and G (2021) Adaptive neural finite-time formation control for multiple under actuated vessels with actuator faults. *Ocean Eng* 222:108556. <https://doi.org/10.1016/j.oceaneng.2020.108556>
- Lai Q, Zeng Q, Zhao X-W, Ge M-F, Xu G (2024) Adaptive finite-time projectivesynchronization of complex networks with nonidentical nodes and quantized time-varying delayed coupling. *Inf Sci* 655:119891. <https://doi.org/10.1016/j.ins.2023.119891>
- Li Q, Yang R, Wang Y, Liu F (2024) Finite-time robust simultaneous stabilization control for two nonlinear singular time-delay systems. *Asian J Control* 26(4):1833-1848. <https://doi.org/10.1002/asjc.3302>
- Liu R, Cao X, Liu M (2017) Finite-time synchronization control of spacecraft formation with network-induced communication delay. *IEEE Access* 5:27242-27253. <https://doi.org/10.1109/ACCESS.2017.2772319>
- Liu Y, Li H, Lu R, Zuo Z, Li X (2022) An overview of finite/fixed-time control and its application in engineering systems. *IEEE/CAA J Autom Sin* 9(12):2106-2120. <https://doi.org/10.1109/JAS.2022.105413>
- Luo Y, Huang W, Cao J, Cao Z (2024) Finite-time consensus of second order multi-agent connectivity preserving based on adaptive sliding mode control. *Commun Nonlinear Sci Numer Simul* 137:108142. <https://doi.org/10.1016/j.cnsns.2024.108142>
- Mikaberidze G, Chowdhury SN, Hastings A, D'Souza RM (2024) Consensus formation among mobile agents in networks of heterogeneous interaction venues. *Chaos Solit Fractals* 178:114298. <https://doi.org/10.1016/j.chaos.2023.114298>
- Moulay E, Dambrine M, Yeganefar N, Perruquetti W (2008) Finite-time stability and stabilization of time-delay systems. *Syst Control Lett* 57(7):561-566. <https://doi.org/10.1016/j.sysconle.2007.12.002>
- Ni J, Hu J, Xiang C (2021) A review for design and dynamics control of unmanned ground vehicle. *Proc Inst Mech Eng Part D* 235(4):1084-1100. <https://doi.org/10.1177/0954407020912097>
- Nie R, Du W, Li Z, He S (2023) Sliding mode-based finite-time consensus tracking control for multi-agent systems under actuator attacks. *Inf Sci* 640:118971. <https://doi.org/10.1016/j.ins.2023.118971>
- Romero JG, Nuno E, Restrepo E, Sarras I (2023) Global consensus-based formation control of non-holonomic mobile robots with time varying delays and without velocity measurements. *IEEE Trans Autom Control* 69(1):355-362. <https://doi.org/10.1109/TAC.2023.3264744>
- Shou Y, Xu B, Lu H, Zhang A, Mei T (2022) Finite-time formation control and obstacle avoidance of multi-agent system with application. *Int J Robust Nonlinear Control* 32(5):2883-2901. <https://doi.org/10.1002/rnc.5641>
- Wang J, Bi C, Wang D, Kuang Q, Wang C (2022) Finite-time distributed event-triggered formation control for quadrotor uavs with experimentation. *ISA Trans* 126:585-596. <https://doi.org/10.1016/j.isatra.2021.07.049>
- Wang J, Yan Y, Liu Z, Chen CP, Zhang C, Chen K (2023) Finite-time consensus control for multi-agent systems with full-state constraints and actuator failures. *Neural Netw* 157:350-363. <https://doi.org/10.1016/j.neunet.2022.10.028>



- Wang X, Li J, Xing J, Wang R (2017) A novel finite-time average consensus protocol based on event-triggered nonlinear control strategy for multiagent systems. *J Inequal Appl* 2017(1):258. <https://doi.org/10.1186/s13660-017-1533-6>
- Wen L, Yu S, Zhao Y, Yan Y (2023) Finite-time dynamic event-triggered consensus of multi-agent systems with disturbances via integral sliding mode. *Int J Control* 96(2):272-281. <https://doi.org/10.1080/00207179.2021.1989045>
- Xie T, Xiong X, Zhang Q (2024) Finite-time synchronization of discontinuous fractional-order complex networks with delays. *IEEE Access* 12:128482-128493. <https://doi.org/10.1109/ACCESS.2024.3430537>
- Xu J, Wang Y, Xing W, Du X, Herrera-Viedma E (2023) Model free finite-time formation containment control of under actuated uavs subject to input delays and unknown interaction information. *Ocean Eng* 283:115054. <https://doi.org/10.1016/j.oceaneng.2023.115054>
- Yakıcı E, Karatas M, Eriskin L, Cicek E (2024) Location and routing of armed unmanned aerial vehicles and carrier platforms against mobile targets. *Comput Oper Res* 169:106727. <https://doi.org/10.1016/j.cor.2024.106727>
- Yang J, Xiao F, Chen T (2020) Event-triggered formation tracking control of non-holonomic mobile robots without velocity measurements. *Automatica* 112:108671. <https://doi.org/10.1016/j.automatica.2019.108671>
- Yang P, Zhang A, Zhou D (2021) Event-triggered finite-time formation control for multiple unmanned aerial vehicles with input saturation. *Int J Control Autom Syst* 19(5):1760-1773. <https://doi.org/10.1007/s12555-019-0833-7>
- Zhang A, Zhou D, Yang M, Yang P (2018) Finite-time formation control for unmanned aerial vehicle swarm system with time-delay and input saturation. *IEEE Access* 7:5853-5864. <https://doi.org/10.1109/ACCESS.2018.2889858>
- Zhang W, Zeng J, Zhang J, Li Z (2022) H consensus tracking of recovery system for multiple unmanned underwater vehicles with switching networks and disturbances. *Ocean Eng* 245:110589. <https://doi.org/10.1016/j.oceaneng.2022.110589>
- Zhao Y, Duan Z, Wen G, Chen G (2016) Distributed finite-time tracking of multiple non-identical second-order nonlinear systems with settling time estimation. *Automatica* 64:86-93. <https://doi.org/10.1016/j.automatica.2015.11.005>
- Zhou D, He L, Cao Z, Zhang A, Han X Event-triggered fixed-time resilient control for mobile sensor networks with Sybil attack and input delay. *Int J Appl Math Comput Sci*. Forthcoming 2025.
- Znidi A, Nouri AS (2024) Decentralized sliding mode control using an event-triggered mechanism for discrete interconnected Hammerstein systems. *Int J Appl Math Comput Sci* 34(3):349-360. <https://doi.org/10.61822/amcs-2024-0025>